Optical high dynamic range acquisition of crack density evolution in cyclic loaded GFRP cross-ply laminates affected by stitching

Bender, J. J.; Glud, J. A.; Lindgaard, E.

Published in:
Composites Part A: Applied Science and Manufacturing

DOI (link to publication from Publisher):
10.1016/j.compositesa.2018.05.032

Publication date:
2018

Document Version
Accepted author manuscript, peer reviewed version

Optical HDR Acquisition of Crack Density Evolution in Cyclic Loaded GFRP Cross-Ply Laminates Affected by Stitching

J.J. Bender, J.A. Glud, E. Lindgaard

PII: S1359-835X(18)30218-5
DOI: https://doi.org/10.1016/j.compositesa.2018.05.032
Reference: JCOMA 5057

To appear in: *Composites: Part A*

Received Date: 11 January 2018
Accepted Date: 28 May 2018

Please cite this article as: Bender, J.J., Glud, J.A., Lindgaard, E., Optical HDR Acquisition of Crack Density Evolution in Cyclic Loaded GFRP Cross-Ply Laminates Affected by Stitching, *Composites: Part A* (2018), doi: https://doi.org/10.1016/j.compositesa.2018.05.032

Optical HDR Acquisition of Crack Density Evolution in Cyclic Loaded GFRP Cross-Ply Laminates Affected by Stitching

J. J. Bender, J. A. Glud and E. Lindgaard
Department of Materials and Production, Aalborg University,
Fibigerstraede 16, 9220 Aalborg East, Denmark

Abstract

The fatigue crack density evolution in a cross-ply laminate where edge finish and stitching are taken into account is investigated. Diamond saw and water jet cutting are used to produce the test specimens and some of the specimens are polished afterwards. The crack density evolution and crack initiations are tracked automatically. It is shown that the number of cracks initiating at the edges for non-polished specimens are similar, whereas the diamond saw cut and polished specimens have fewer cracks at the edges, and the water jet cut and polished specimens have even fewer. In addition it is shown that the crack density is higher in the stitching areas than in the rest for polished specimens. This indicates that the stitching is highly governing of where cracks initiate and propagate in the specimens with limited edge defects. The same applies to real composite structures, which are negligibly affected by edge defects.

Keywords: *Glass fibres, Transverse cracking, Fatigue, Cutting*

1. Introduction

Wind turbine blades (WTBs) are becoming bigger every year and often when the blade size is increased a new type certification is required. This certification can be obtained by complying with the design practice published by a certification body, e.g. DNVGL.

According to the DNVGL-ST-0376 standard [1], it is required that WTBs are designed against off-axis matrix cracks or Inter Fibre Failure (IFF) cracks using e.g. Pucks criterion [2]. These IFF cracks may be a design driver and hereby require reinforcement of the blade to comply with the standard. The Puck criterion relies on the transverse strength of the unidirectional (UD) layers used in the blade, which are obtained through testing of pure UD layers [3]. However, a WTB consists of laminates with layers in many directions, therefore, the constraining effect of the adjacent layers increases the apparent transverse strength of the UD layers as described in [4,5]. It is also shown in [6] for the fatigue case that the number of cycles to crack initiation is increased due to the constraining effect of layers in the load direction.

With higher transverse strength design values, less reinforcement is required, meaning a lower weight of the blade. Therefore, it is of great interest to obtain UD transverse strengths when the UD layers are embedded in a laminate. However, when testing laminates, the edge effect and defects induced by the cutting of the specimens may pollute the results and reduce the apparent strength. An indication that the edges affect the results is that most cracks during testing initiate from the edges [7–11]. The defects from cutting are usually considered alleviated by polishing the edges of the specimens [12–16]. However, very few studies have focused on the effect of the cutting technique prior to the polishing, and especially regarding fatigue. In [17,18] it is shown for static tensile tests that the strain at first crack onset is increased when diamond saw cut specimens are polished.

Today, more advanced cutting techniques such as water jet cutting is used when preparing specimens [11,19,20]. Specimens for static or fatigue testing cut with water jet are generally not polished afterwards. To the knowledge of the authors, it has not been investigated previously if the polishing after water jet cutting affects the static or fatigue properties.

Water jet cut specimens without subsequent polishing exhibit a very large scatter of two orders of magnitude in fatigue results regarding the number of cycles for off-axis crack initiation in multi directional laminates [11]. This means that when pure UD layers are tested, only the absolute weakest points are found and used to characterise the material. This is a conservative estimate of the actual properties of the material, thus leading to a conservative design. To design for anything other than the first off-axis crack requires information on the statistical distribution of the material properties. With a new technique developed by Glud et al. in [21], it is possible to obtain this statistical distribution with few test specimens. The Automatic Crack Counting (ACC) algorithm presented in [21] can detect all visible initiating cracks in a measuring area and track the propagation of these. Furthermore, this data can be used to accurately measure the crack density evolution in the measuring area and correlate this to a loss of stiffness for the specific lay-up. The crack density is obtained automatically meaning that the results are reproducible and not prone to human error as these measurements usually are. This makes crack density a much more viable metric for quantifying the damage state of composites.

Models have been developed where the crack density is used to predict the damage state of an arbitrary lay-up e.g. in ref [22–29]. When these models are further matured, it is possible to accurately predict the stiffness degradation of an arbitrary lay-up based on the crack density in the laminate. This allows for an accurate estimation of the structural integrity after IFF cracks have occurred in e.g. a WTB. It is the opinion of the authors of this work that these types of models with further maturing can be used to certify new WTBs with minor modifications to the guidelines in the DNVGL-ST-0376 standard. The modifications are already underway, because in the DNVGL-ST-0376 it is possible to obtain the type certification if it can be shown that IFF cracks sustained during testing do not affect the structural integrity of the WTB.

If crack density is to be used in a certifying context then it is necessary to understand which parameters influence the evolution of the crack density. The fibre mats used to manufacture WTBs are usually non-crimp-fabrics (NCF) where bundles of fibres in layers are stitched together and bundles of backing fibres in layers are used as well to ensure that the primary fibres keep their orientation. Backing layers are thin bundles of fibres on the backside of a fabric oriented at $\approx 90^\circ$ to the rolling direction. Backing layers are particularly used when the fabrics are draped on steep curved surfaces [30]. It has been shown that the backing layers of the NCF fabrics have a large influence on when and where damage initiates and final failure occurs during fatigue testing of quasi UD laminates where only the backing layers are not parallel to the load direction [30–32]. In [30,31] there are also indications that off-axis matrix cracks initiate in the vicinity of stitching meaning that the stitching thread may act as an initiator of these cracks. The off-

axis matrix cracks can in turn lead to local concentrations of fibre breaks especially in GFRP. Cross-ply laminates without backing layers were tested in [33] with the focus of relating the void content to a reduction in tensile and compressive strength. Most off-axis matrix cracks initiated from voids and a few initiated in areas with stitching. Typically in the cited works [30–33], the fibre breakages are localized in the vicinity of off-axis matrix cracks no matter if the cracks initiated from voids, backing layers, stitching, or off-axis layers. This indicates that any fibrous material not parallel to the load direction can act as initiators of Inter Fibre Failure (IFF), which causes localization of fibre breakage of load bearing fibres leading to final failure.

From this it is apparent that the backing and to some extent the stitching affects crack initiations, however, the crack density has not been considered in any of the cited works. Furthermore, the effect of the cutting technique on the crack density evolution through a fatigue test has not been considered. This leads to the following research questions, which are dealt with in this paper.

- Is the effect of the edge defects on the fatigue damage evolution different for specimens cut with water jet and diamond saw, respectively?
- Does polishing affect the fatigue damage evolution differently for specimens cut with water jet and diamond saw, respectively?
- Are the damages that occur in laminated composite structures e.g. wind turbine blades affected by the stitching in the NCF?

2. Specimen manufacturing and test setup

The specimen constituents and manufacturing process are described, followed by a description of the test setup and the post-processing routine based on the ACC algorithm with emphasis on the newly developed parts.

2.1 Specimen manufacturing

The laminate used in this work is manufactured from Uniaxial 661 g/m2 H-glass fibres with a matrix consisting of GT 105 Polyester through a Vacuum Assisted Resin Transfer Moulding process. The dry fibre mats are shown in Fig. 1 and in (a) the backing fibre bundles are shown, which are in a $\pm 80^\circ$ pattern with approximately 8 wt%. The backing bundles are attached to the fibre bundles with a polyester stitching thread in a pattern as shown in Fig. 1(a,b).

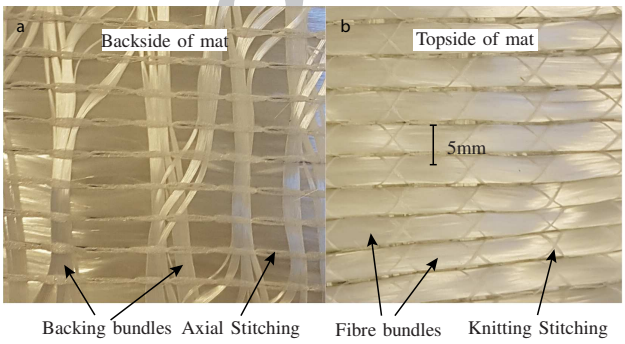

Fig. 1 Images of the dry fibre mats with stitching pattern used to manufacture the specimens.

The lay-up used in this work is $[0,90]_S$ where the backing layers are turned toward the outside of the laminate meaning that the 90 degree layer effectively has double thickness compared to the individual constraining layers, as shown in Fig. 2. The individual layers are 0.55mm thick, and the total thickness is 2.2mm. During infusion, the laminate is placed on a glass table to get a smooth surface to be able to detect the changes in light transmitted through

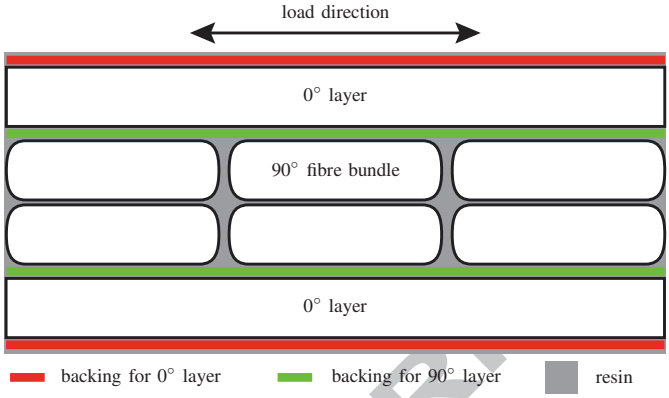

Fig. 2 Illustration of the tested lay-up.

the specimen during testing. End tabs made from GFRP are attached to the laminate after the infusion, and the specimens are cut using two different cutting techniques, where the final dimensions are shown in Fig. 3. 6 specimens are cut with a Diamond Saw (DS) and 6 are cut with Water Jet (WJ). Four of each of these specimen types are polished afterwards yielding two groups more, namely, Diamond Saw polished (DSp) and Water Jet polished (WJp). The polishing is done manually on a 'Struers Tegramin-30' with increasingly finer grain size down to 1μm.

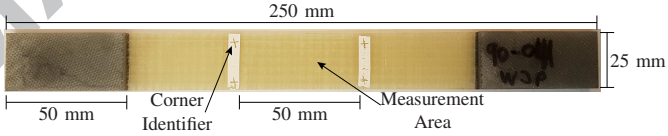

Fig. 3 Image of one of the tested specimens with final dimensions.

2.2 Test Setup

The fatigue tests are performed in an Instron ElectroPuls E1000 with load control in Tension-Tension with an R-ratio of 0.1 with maximum load at 90% of the static transverse strength of the pure quasi UD with backing. Two light sources are used to illuminate the front and to transluminate the specimen from the back, respectively, as shown in Fig. 4. A 5MP Blackfly camera is used during testing to capture the initiation and propagation of cracks in the measurement area. The camera can detect the cracks during testing when the cracks appear because they disrupt the light transmitted through the material which makes the crack area darker than before. The test is run for intervals of 15, 50, and 500 cycles for 4.500, 60.000, and ≈600.000, respectively. After each interval the test is stopped at an unloaded state to capture three images in a row with varying shutter speeds to account for variations in light intensity in the specimen.

2.3 Automatic Crack Counting Algorithm

After testing, the images are post-processed as described in [21] with a few modifications as indicated in the list below, where the parts in bold are specific for the algorithm used in this work:

1) Capture single image / **Capture three images**
2) Motion compensation
3) **Determination and application of weighting matrix**
4) Divide image by undamaged
5) Filtering
6) Crack counting

The steps described above are also shown in Fig. 5 with samples of the used images. In the original algorithm, one image is captured at

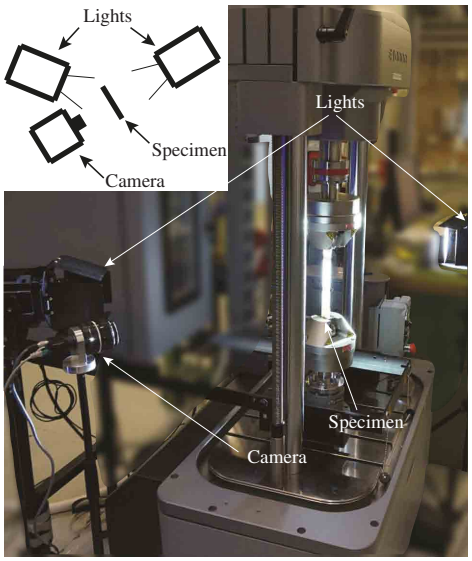

Fig. 4 The test setup is shown with a schematic in the top left.

every interval and used in the motion compensation, and in this work, three images are captured and motion compensation is performed before they are combined into one. This step is a necessity as shown in Fig. 5(a-b) because the clearly visible cracks in (b) are almost impossible to detect in (a). The three images are combined by weighting them based on the greyscale value, which is comparable to the technique used when making High Dynamic Range (HDR) images, which is why the combined images are henceforth referred to as HDR-images. The algorithm is described in the following, with emphasis on the newly developed parts.

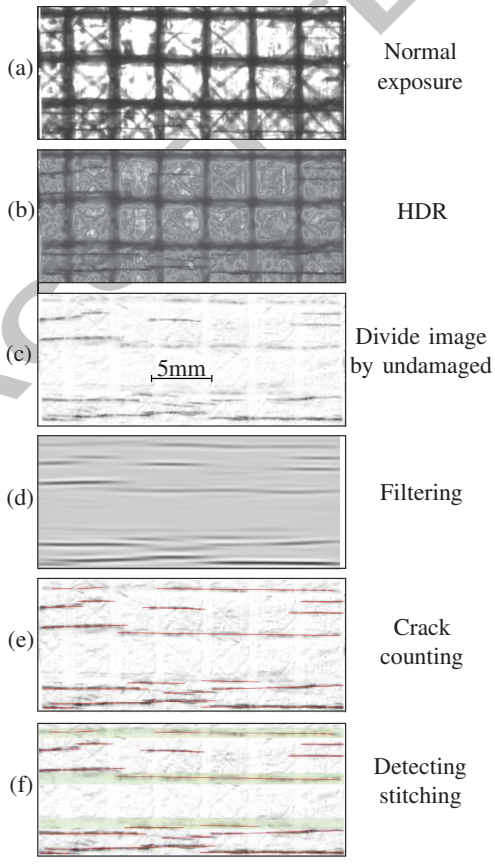

Fig. 5 Sample of the stages through the ACC algorithm.

Capture Three Images

The fatigue test is paused and unloaded and three images are captured with different shutter speeds. Samples of these images are shown in Fig. 6.

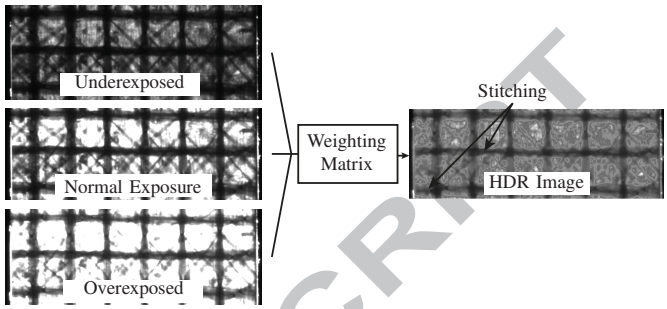

Fig. 6 Sample of images with three different shutter speeds, and the combined HDR image.

One images is underexposed in such a manner that there are no overexposed pixels. One image is overexposed so that the greyscale value in the stitching is increased to a level where it is possible to detect cracks. The last image is captured with a shutter speed in between the two others to ensure a smooth transition in the HDR-image in the areas of high greyscale gradients. The motion compensation is calculated as in the original algorithm by using the corner identifiers as shown in Fig. 7.

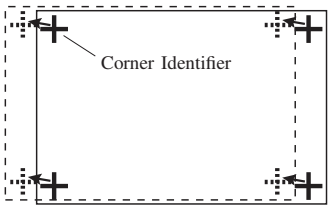

Fig. 7 Motion compensation aligns the corner identifiers from the damaged image (solid lines) with the undamaged image (dashed lines).

However, the motion compensation is only calculated for one of the three images at each interval and the resulting movements and rotations are then used for the other two images at each interval.

Determination and Application of Weighting Matrix

Through the weighting matrix the three images with varying shutter speeds are combined with each other. The matrix is only calculated once, which is before the first interval of cycles in the test. The weighting is done by considering the greyscale value of each pixel in the image with normal exposure. If the greyscale value in a pixel is below half of the maximum then the corresponding pixel value in the HDR image is a weighted sum of the normal- and overexposed images. Similarly, if the greyscale value is above half then the weighted sum is between the normal- and underexposed images. The weighting is based on a sine-function as shown in Fig. 8.

When cracks appear, the greyscale value decreases, but the determination of the weighting is only done for the first three images and applied to all the other images, so the cracks are not washed out because the images are weighted similarly, and cracks can be seen as in Fig. 5(b). This however, underlines the importance of doing motion compensation before creating the HDR images, because if the images are shifted a few pixels in any direction the resulting pixel values in the HDR image could be a combination of two wrong images. This is especially a concern in the areas with high greyscale gradients, because artificial crack-like shapes can be the outcome of improper motion compensation which then pollutes the result.

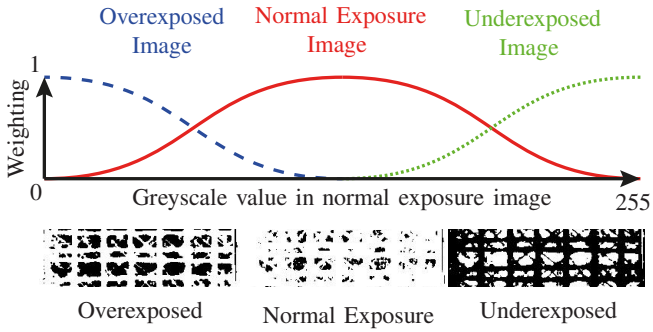

Fig. 8 The top image indicates the weighting of each image based on the greyscale value in the image with normal exposure for every pixel, the bottom 3 images indicate with white, which pixel values from the 3 images are used to create the HDR image.

After the HDR images are created, they are divided by the undamaged HDR image pixel by pixel. This means that if the greyscale value in a given pixel is the same for two consecutive images, then the resulting pixel value in the resulting image is 255 because the division, which is equal to 1, is converted into a greyscale value. This leaves a white background where no changes occur, and black lines where the cracks are, as shown in Fig. 5(c). From this figure it is apparent that the cracks are darker and more easily detectable when they are not in the stitching. A microscopic analysis of the edge of a specimen is performed after fatigue testing to verify that the dark lines in the stitching and out of the stitching are caused by similar cracks. The results are shown in the next section. The images from Fig. 5(c) are then filtered as shown in Fig. 5(d) and reduced to binary images. In the binary images the cracks are counted, their end points are found, and the cracks are drawn and overlayed on the images as shown in Fig. 5(e). The overlayed image enable easy manual inspection that the cracks are detected satisfactorily. The total combined crack length can be determined when the end points of all the cracks are known, and this can in turn be used to calculate the crack density. In this work the crack density is defined in the same manner as in [21], which is shown in Eq. 1.

$$CD = \frac{\Sigma_{i=1}^{n} L^i}{A_{\text{measure}}} \tag{1}$$

Where L^i is the length of the i'th crack, and A_{measure} is the measuring area. The crack density in the stitching areas is of interest in this work. Therefore, these areas have to be quantified based on the change in greyscale value in the vertical direction of the undamaged image as indicated by the green areas in Fig. 5(f). The crack density related to the stitching areas can then be calculated as shown in Eq. 2.

$$CD_{\text{stitch}} = \frac{L_{\text{stitch}}}{A_{\text{stitch}}} \qquad CD_{\text{rest}} = \frac{L_{\text{rest}}}{A_{\text{measure}} - A_{\text{stitch}}} \tag{2}$$

Where L_{stitch} is the total length of cracks in the stitching areas, L_{rest} is the total length of cracks in the rest of the measuring area, A_{stitch} is the combined stitching area, and CD_{stitch} and CD_{rest} are the crack densities in the stitching area and in the rest of the measuring area, respectively.

3. Experimental Results

The experimental results are divided into three parts. The first part is focused on showing that the changes in greyscale value that occur in the stitching and in the rest of the measuring area represent the same type of damage. This is done by comparing micrographs from the edge of a specimen at stitching areas and away from stitching areas. In the second part, data is presented to show the effect of the cutting technique on the number of cracks initiating at the edges and on the average number of cycles to isolated crack initiations meaning that there is more than four times the thickness of the cracking layer between the cracks [10]. The last part compares the crack density evolution in the stitching areas and in the rest of the specimen for polished and non-polished specimens.

3.1 Micrographs

After testing, the edges of the specimens were examined with a Scanning Electron Microscope (SEM) to determine possible differences between cracks in the stitching areas and in the rest of the specimen. As shown in Fig. 9 a crack in the stitching goes all the way from the $\pm 80^\circ$ backing in the top to the $\pm 80^\circ$ backing in the bottom, the same goes for cracks in the rest of the specimen as shown in Fig. 10. In the micrographs all the cracks going from top to bottom of the off-axis layers are in areas with knitting stitching. This means that it is likely that the cracks initiate at the interface between the stitching thread and the polyester and from there propagate to the backing layers. This indicates that the backing layers arrest off-axis

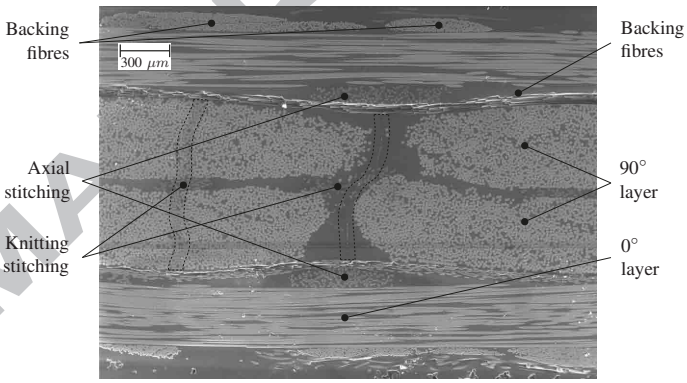

Fig. 9 Micrograph of the edge of a WJp specimen with a crack in a stitching area and next to it (the cracks are indicated by the dashed boxes).

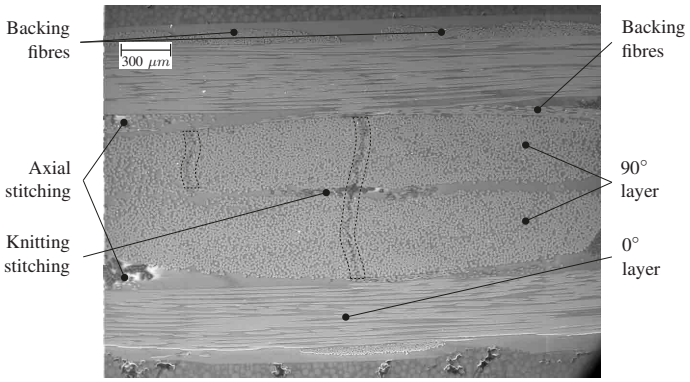

Fig. 10 Micrograph of the edge of a WJp specimen with two cracks outside of the stitching area, where one goes through the entire thickness of the off-axis layers (the cracks are indicated by the dashed boxes).

crack development instead of promoting it, which was shown to be the case in [30–32]. In these cited works the backing layers were the layers with the largest angle w.r.t. the load direction whereas in this work the off-axis layers and the stitching are at an angle of 90° and the backing is at $\pm 80^\circ$. This suggests that the angle of the off-axis fibrous material is more important than the mechanical- and interfacial-properties of it.

3.2 Edge cracks affected by cutting technique

As described, the specimens have been cut using different techniques and some of them have been polished afterwards in order

to investigate the effect of the polishing after cutting. The possible influence of the polishing and cutting technique should be determined before the effect of the stitching can be considered. Through the cutting technique, it is only possible to affect the crack initiations at the edges, therefore, the number of cycles until isolated crack initiation at the edges is considered. Furthermore, the number of cracks initiating at the edges compared to the total number of cracks in the specimens is considered as well. This is done because, as it is shown in Fig. 11, the number of cycles until isolated crack initiation is not an appropriate measure of the effect of the edges due to high scatter in the data.

Fig. 11 shows box plots of the number of cycles for an isolated crack to initiate in the entire measurement area (shown in blue) and only at the edges (shown in green). The data is sorted into four groups based on the cutting and polishing, and the distribution of the data in the groups is indicated by separate box plots. There are 20-40 data points for the blue boxes and 10-20 for the green boxes. For all the groups the main part of the isolated cracks initiate early in the test, before 6000 cycles. It also seems that the cracks initiate earlier at the edges and with less scatter than in the rest of the measurement area. However, the scatter within the groups is very high, therefore, it is not statistically significant to conclude that cracks initiate earlier or later based on edge finish. The high scatter within these groups of similar specimens indicates that inherent differences between the specimens i.e. defects such as dry fibres, fibre waviness, micro voids, etc. highly affect when the cracks initiate [34]. This also means that the cutting technique and polishing only has a minor effect on when cracks initiate, if any.

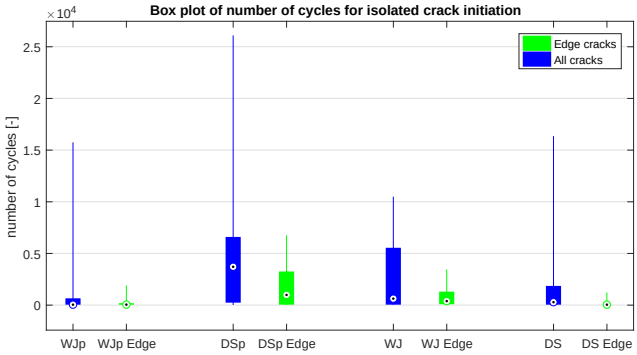

Fig. 11 Box plots showing the distribution of the number of cycles to crack initiation based on isolated cracks for the four groups of specimens for cracks everywhere (about 10 cracks per specimen) and for edge cracks (about 5 cracks per specimen). The black dots indicate the median, the lower and upper edges of the boxes indicate the 25th and 75th percentile, respectively, and the lines represent the minimum and maximum values of the data.

However, the scatter is a lot smaller if the number of cycles until crack initiation is neglected and only the number of cracks at the edges is considered. This is shown in Fig. 12 where a difference is apparent in the number of cracks initiating at the edges compared to the total number of cracks depending on the cutting technique, henceforth this ratio is called edge ratio. There are two sets of results in Fig. 12 the blue boxes show the results when all the cracks are counted, and the green boxes show the results when only isolated cracks are counted. The trend between the groups is the same whether all cracks or just the isolated cracks are considered. However, the variance is higher for the isolated cracks because the calculations are based on fewer cracks.

The two polished groups have a significantly lower edge ratio compared to the non-polished groups. The WJp-group has an even lower edge ratio compared to the DSp-group. Both groups have been polished for the same duration and with the same grain sizes meaning that the same amount of material has been removed. Therefore, the difference in edge ratio indicates that the diamond saw cutting technique affects the specimen deeper and these effects are not removed completely with the applied polishing, as illustrated in Fig. 13. For non-polished specimens, there is no significant difference in edge ratio between water jet cutting and diamond saw cutting. The lack of

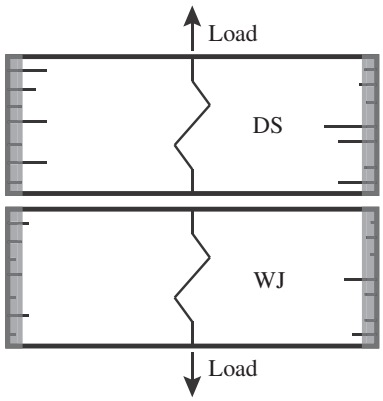

Fig. 13 Illustrative front view of two different specimens with initial edge defects from cutting, where the grey area indicates the area that will be removed during polishing. The specimens are considered to have the same number of defects, but they are deeper in the DS specimen.

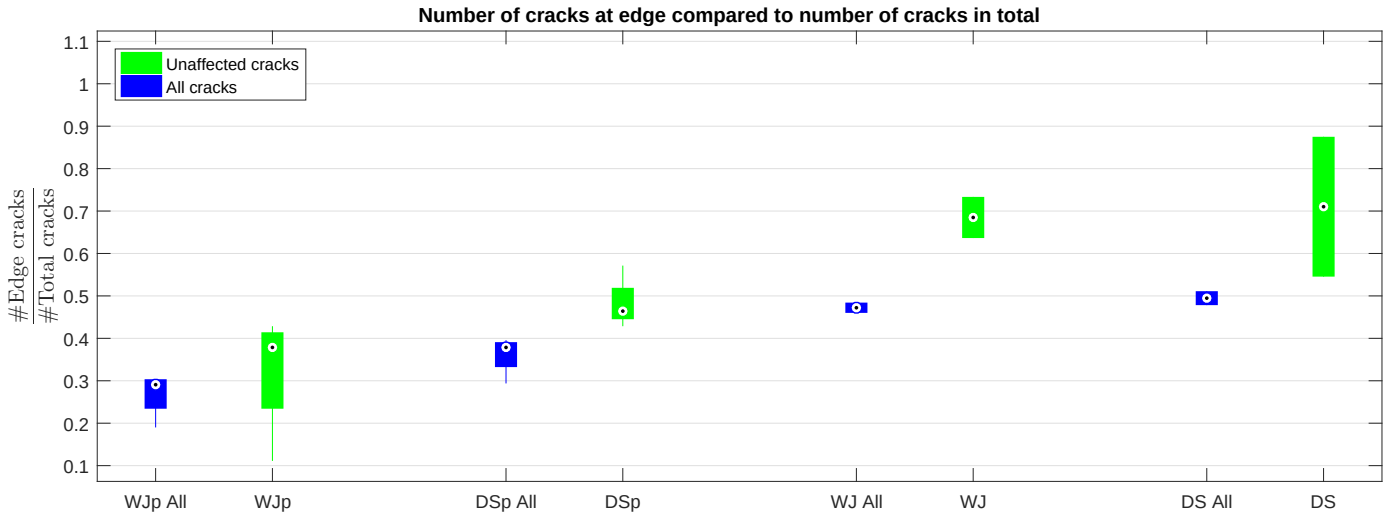

Fig. 12 Box plots of ratio of cracks initiating at the edges to total number of cracks after 500.000 cycles.

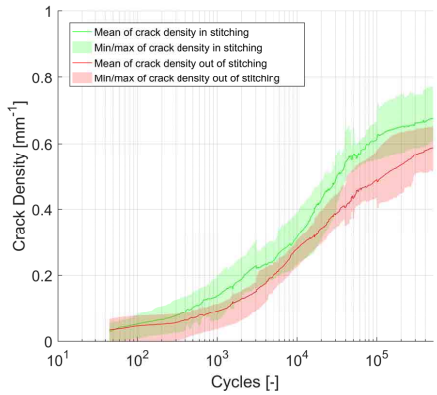

Fig. 14 The crack density evolution for WJ and DS specimens in the axial stitching area and out of the axial stitching area.

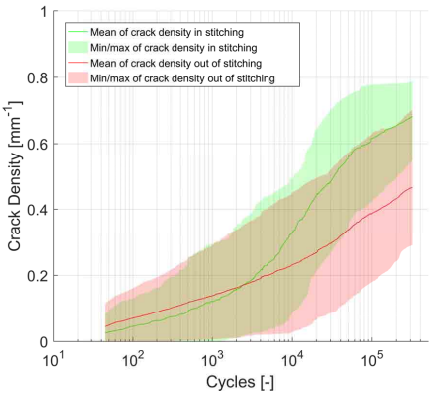

Fig. 15 The crack density evolution for DSp specimens in the axial stitching area and out of the axial stitching area.

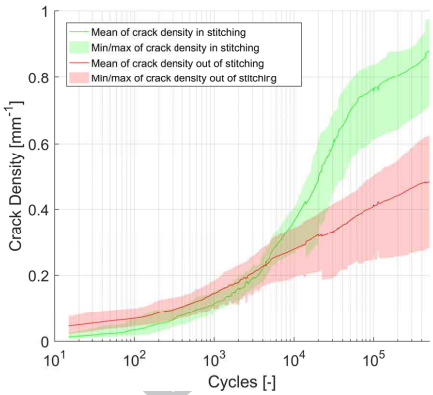

Fig. 16 The crack density evolution for WJp specimens in the axial stitching area and out of the axial stitching area.

difference between the two non-polished groups in Fig. 12 indicates that the depth of the defects has no influence on the probability of initiation of edge cracks. This is supported by the findings in [18] where it was found that cross-ply laminates were insensitive to the depth of notches. Furthermore, in [20] both WJ and DS was used to cut specimens without polishing and no difference between the two cutting techniques for static and fatigue tests was reported. If there is a defect, there is an increased probability of a crack.

The results in this section show that the cutting technique and the polishing has an effect on the initiation of edge cracks. However, the effect is limited to the edge ratio and not *when* the cracks initiate in the specimens. This is most likely because the polishing removes most of the edge defects, but those that remain influence the results in the same manner as before, i.e. the cracks will initiate after the same number of cycles, only there are fewer of them. Based on the data in Fig. 12 three groups are considered further on for analyzing the crack density in the stitching areas and in the rest of each of the specimens.

- The non-polished specimens (WJ and DS)
- The polished diamond saw cut specimens (DSp)
- The polished water jet cut specimens (WJp)

The WJ and DS specimens are considered as one group because they have similar edge ratios, and the crack density evolution is similar, as shown in the next section. The DSp and WJp are considered as two different groups because they have different edge ratios, which will most likely influence the crack density evolution.

3.3 Crack density affected by stitching

In the following, the crack density evolution is considered for the three groups. The crack density is accounted for in the axial stitching areas, i.e. the green areas in Fig. 5(d), and in the rest of the specimen. These two evolutions are compared within the groups to detect changes in the evolution due to the stitching. The crack density evolution is determined for each individual specimen, and the average crack density for each group at each cycle interval is then calculated and plotted in the following section with associated standard deviations.

In Fig. 14 the crack density evolution for the non-polished specimens is shown and it can be observed that there is no significant difference between the crack density in and out of the axial stitching areas throughout the entire fatigue test. Furthermore, the sigmoidal shape of the crack density evolution is similar to that found in literature [34–37].

However, for the polished diamond saw cut specimens in Fig. 15 the trend looks different even with a high deviation in the results. At ≈4000 cycles the crack density in the axial stitching area increases more rapidly as expected based on the sigmoidal shape. 4000 cycles is close to the median value of the number of cycles to crack initiation, meaning that more than half of the isolated cracks have initiated at this time during the fatigue test. The crack density evolution outside the axial stitching area does not have a sigmoidal shape, which is discussed later.

For the polished water jet cut specimens, the trend is even more noticeable in Fig. 16. There is a significant difference in crack density in and out of the axial stitching area after ≈20000 cycles. The trend for WJp specimens and DSp specimens is similar, at ≈4000 cycles the crack density in the axial stitching area increases more rapidly. Moreover, for the WJp specimens the increase in crack density is a lot higher than for the DSp specimens. The crack density evolution out of the axial stitching area is not a sigmoidal shape, which was also the case for the DSp specimens.

It is shown that the non-polished specimens have insignificantly different crack densities in and out of the axial stitching areas for the entire fatigue test. However, the polished specimens have different crack density evolution trends in and out of axial stitching area, resulting in significantly higher crack densities in the axial stitching areas for WJp specimens after ≈20000 cycles. The deviation is too large for the DSp specimens to state that there is a significant difference between the crack density in and out of the axial stitching area, but it seems to be the case.

4. Discussion

The general sigmoidal trend of the crack density evolution is common in the literature [34–37]. This trend has been divided into three phases as shown in [9] and summarized below:

1) The crack density evolution is slow because only a few cracks have initiated at locations of low strength and/or high stress i.e. voids, stitchings, and defects caused by the cutting of the edges.
2) The slope of the crack density evolution increases as the median of the number of cycles to isolated crack initiation is approached, therefore, more cracks are initiating and propagating.
3) The crack density evolution slows down again as the cracks have reached the edges and cannot propagate anymore, and no new cracks are initiated. A crack density saturation has been reached.

From the results regarding non-polished specimens in the previous section it is observed that the crack density evolution follows the

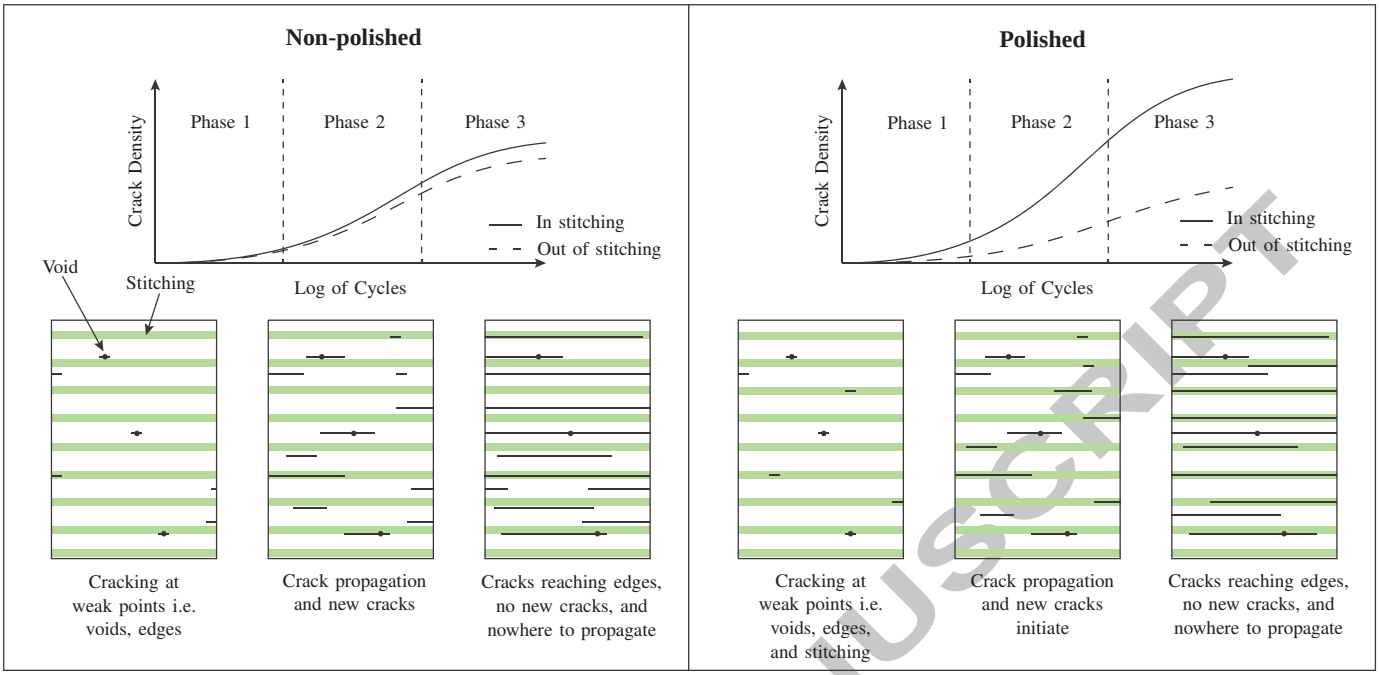

Fig. 17 Hypothesized phases of the crack density evolution, for the non-polished specimens the crack density evolution is similar in and outside of the stitching. The first cracks initiate at defects, such as voids and edges. Then cracks initiate at more locations and start to propagate. Finally, the cracks reach the edges and the entire volume is unloaded due to cracks, so no more cracks are initiating.

trend from the literature and the crack density is almost the same in and out of the stitching. This means that for non-polished specimens, the stitching does not influence where the cracks initiate and propagate. This is illustrated in Fig. 17, where the crack density evolution follows the three phases as described above. In the first phase the first cracks initiate at locations with local stress concentrations such as voids and cutting defects at the edges. These early cracks reduce the stress level on either side of them as described in [38]. In the second phase cracks initiate at locations where there are no defects but the stress is high i.e. far away from cracked areas. This leads to an increase in crack initiations and an increase in the slope of the crack density evolution. In the third phase almost all cracks are interacting and most have propagated across the entire specimen, which leads to a decrease in the number of crack initiations and decrease in crack propagation, and hereby a decrease in the slope of the crack density evolution. Since the crack density in and out of the stitching is similar, the cracks are evenly distributed over the entire measurement area regardless of the stitching.

The results from the polished specimens show a different behaviour. There is a significantly higher crack density in the stitching, and the crack density out of the stitching does not follow the sigmoidal shape, which is unexpected based on the literature. This indicates that there is an increase in total crack length in the stitching areas as a result of more and/or longer cracks. Furthermore, there seems to be a decrease in the crack density out of the stitching. In the following a hypothesis is presented that explains this behaviour, and it is also illustrated in Fig. 17.

The only difference between the polished and the non-polished specimens is the edges, and therefore, the reason for the difference in crack density evolution has to be found at the edges. As stated before, the crack density evolution is divided in three phases, and in the first phase, the cracks initiate from areas with local stress concentrations. For the non-polished specimens many cracks initiate from the edges at random locations and fewer initiate from edges for the polished specimens (Fig. 12). This is because the defects from the cutting act as local stress concentrators, and as described earlier, most of these stress concentrators are removed during the polishing. Since most local stress concentrators at the edges are removed in the polishing, the cracks initiate at other areas where the strength is low and/or the stress is high, this could be at the stitching. The stitching areas are located with approximately 4 times the thickness of the cracking layer between them meaning that the entire area between the stitching is unloaded as described in [34] when a crack is present in either of the stitching areas. This means that there is a higher probability of crack initiation in the next stitching than between two stitchings when one of them is cracked. Therefore, this effect is self enhancing, which is why there is such a big difference in the crack density for polished specimens and especially WJp where there are the fewest edge cracks.

Laminates in composite structures and WTB are not affected by free edge effects or edge defects, meaning that the WJp results which were the least affected by the edges are most representative of the damage evolution in a WTB. It stands to reason that stitching areas in a WTB have a higher probability of cracking and possibly earlier than non-stitching areas since the stitching in the WJp specimens exhibited significantly higher crack densities than the rest of the specimens.

5. Conclusion

The damage evolution in cross-ply laminates has been studied through the crack density evolution while considering the effect of edge defects and stitchings. The following conclusions are drawn based on the stated research questions:

- The WJ and DS specimens exhibited the same number of initiating cracks at the edges compared to the total number of initiating cracks in the specimens. Furthermore, the crack density evolution was similar for DS and WJ specimens leading to the conclusion that the cutting technique by itself does not change the probability of edge cracks.
- The number of cracks initiating at the edges was significantly reduced when the specimens were polished after cutting. This was the case both for WJp and DSp, however, the effect was significantly higher for the WJp specimens. The difference

is believed to be caused by deeper edge defects in the DS specimens, which are not removed completely by the applied polishing.

- It has been shown that the crack density was significantly higher in the stitching areas for the WJp specimens, which are most comparable to actual composite structures, i.e. WTBs, because these were the least affected by the edges. This also means that stitchings in a composite structure will most likely act as off-axis crack initiators.

From this work and the literature it is clear that stitching and backing fibres both can act as crack initiators, but in this work the backing did not seem to affect the results at all. It is hypothesized that the angle of the off-axis fibrous material is one of the most important factors for the location of off-axis crack initiation, which should be studied in the future.

Acknowledgement

This work was supported by the Innovation Fund Denmark project OPTI_MADE_BLADE, grant no. 75-2014-3. This support is gratefully acknowledged.

References

[1] DNV-GL, "DNVGL-ST-0376 Rotor blades for wind turbines," Tech. Rep. December, 2015. [Online]. Available: http://www.dnvgl.com

[2] A. Puck and H. Schürmann, "Failure analysis of FRP laminates by means of physically based phenomenological models," *Composites Science and Technology*, vol. 62, no. 12-13, pp. 1633–1662, 2002. [Online]. Available: http://www.sciencedirect.com/science/article/pii/S0266353801002081

[3] A. Puck, J. Kopp, and M. Knops, "Guidelines for the determination of the parameters in Puck's action plane strength criterion," *Composites Science and Technology*, vol. 62, no. 3, pp. 371–378, 2002. [Online]. Available: http://www.sciencedirect.com/science/article/pii/S0266353801002020

[4] A. Parvizi and J. E. Bailey, "On multiple transverse cracking in glass fibre epoxy cross-ply laminates," *Journal of Materials Science*, vol. 13, no. 10, pp. 2131–2136, 1978.

[5] D. L. Flaggs and M. H. Kural, "Experimental Determination of the In Situ Transverse Lamina Strength in Graphite/Epoxy Laminates," *Journal of Composite Materials*, vol. 16, no. 2, pp. 103–116, 1982. [Online]. Available: http://journals.sagepub.com/doi/10.1177/002199838201600203

[6] M. Quaresimin and P. A. Carraro, "Damage initiation and evolution in glass/epoxy tubes subjected to combined tension-torsion fatigue loading," *International Journal of Fatigue*, vol. 63, pp. 25–35, 2014. [Online]. Available: http://dx.doi.org/10.1016/j.ijfatigue.2014.01.002

[7] J. Tong, F. J. Guild, S. L. Ogin, and P. A. Smith, "Off-axis Fatigue Crack Growth and the Associated Energy Release Rate in Composite Laminates," *Applied Composite Materials*, vol. 4, no. 5, pp. 349–359, 1997.

[8] T. Yokozeki, Y. Hayashi, T. Ishikawa, and T. Aoki, "Edge effect on the damage development of CFRP," *Advanced Composite Materials*, vol. 10, no. 4, pp. 369–376, 2001.

[9] J. Tong, "Three Stages of Fatigue Crack Growth in GFRP Composite Laminates," *Journal of Engineering Materials and Technology*, vol. 123, no. 1, pp. 139–143, 2001.

[10] M. Quaresimin, P. A. Carraro, L. P. Mikkelsen, N. Lucato, L. Vivian, P. Brøndsted, B. F. Sørensen, J. Varna, and R. Talreja, "Damage evolution under cyclic multiaxial stress state: A comparative analysis between glass/epoxy laminates and tubes," *Composites Part B: Engineering*, vol. 61, pp. 282–290, may 2014. [Online]. Available: http://www.sciencedirect.com/science/article/pii/S1359836814000663

[11] J. A. Glud, J. M. Dulieu-Barton, O. T. Thomsen, and L. C. T. Overgaard, "Fatigue damage evolution in GFRP laminates with constrained off-axis plies," *Composites Part A: Applied Science and Manufacturing*, vol. 95, pp. 359–369, 2017. [Online]. Available: http://dx.doi.org/10.1016/j.compositesa.2017.02.005

[12] E. K. Gamstedt and R. Talreja, "Fatigue damage mechanisms in unidirectional carbon-fibre-reinforced plastics," *Journal of Materials Science*, vol. 34, no. 11, pp. 2535–2546, 1999.

[13] A. W. Wharmby, F. Ellyin, and J. D. Wolodko, "Observations on damage development in fibre reinforced polymer laminates under cyclic loading," *International Journal of Fatigue*, vol. 25, no. 5, pp. 437–446, 2003.

[14] A. Gagel, D. Lange, and K. Schulte, "On the relation between crack densities, stiffness degradation, and surface temperature distribution of tensile fatigue loaded glass-fibre non-crimp-fabric reinforced epoxy," *Composites Part A: Applied Science and Manufacturing*, vol. 37, no. 2, pp. 222–228, 2006.

[15] J. Andersons, R. Joffe, and E. Spārniņš, "Statistical model of the transverse ply cracking in cross-ply laminates by strength and fracture toughness based failure criteria," *Engineering Fracture Mechanics*, vol. 75, no. 9, pp. 2651–2665, 2008. [Online]. Available: http://linkinghub.elsevier.com/retrieve/pii/S0013794407001117

[16] L. Zubillaga, A. Turon, J. Renart, J. Costa, and P. Linde, "An experimental study on matrix crack induced delamination in composite laminates," *Composite Structures*, vol. 127, pp. 10–17, 2015. [Online]. Available: http://linkinghub.elsevier.com/retrieve/pii/S0263822315001658

[17] A. Kitano, K. Yoshioka, K. Noguchi, and J. Matsui, "Edge Finishing Effects on Transverse Cracking of Cross-Ply CFRP Laminates," in *Proceedings International Conference on Composite Materials 9 Vol 5*, A. Miravete, Ed. Madrid: University of Zaragoza, 1993, pp. 169–176.

[18] L. E. Crocker, S. L. Ogin, P. A. Smith, and P. S. Hill, "Intra-laminar fracture in angle-ply laminates," *Composites Part A: Applied Science and Manufacturing*, vol. 28, pp. 839–846, 1997.

[19] B. Stier, J. W. Simon, and S. Reese, "Finite Element Analysis of Layered Fiber Composite Structures Accounting for the Material's Microstructure and Delamination," *Applied Composite Materials*, pp. 171–187, 2014.

[20] K. Vallons, G. Adolphs, P. Lucas, S. V. Lomov, and I. Verpoest, "The influence of the stitching pattern on the internal geometry, quasi-static and fatigue mechanical properties of glass fibre non-crimp fabric composites," *Composites Part A: Applied Science and Manufacturing*, vol. 56, pp. 272–279, 2014. [Online]. Available: http://dx.doi.org/10.1016/j.compositesa.2013.10.015

[21] J. Glud, J. M. Dulieu-Barton, O. T. Thomsen, and L. C. T. Overgaard, "Automated counting of off-axis tunnelling cracks using digital image processing," *Composites Science and Technology*, vol. 125, pp. 80–89, 2016. [Online]. Available: http://dx.doi.org/10.1016/j.compscitech.2016.01.019

[22] P. Lundmark and J. Varna, "Constitutive Relationships for Laminates with Ply Cracks in In-plane Loading," *International Journal of Damage Mechanics*, vol. 14, no. 3, pp. 235–259, 2005. [Online]. Available: http://journals.sagepub.com/doi/10.1177/1056789505050355

[23] P. Lundmark and J. Varna, "Crack face sliding effect on stiffness of laminates with ply cracks," *Composites Science and Technology*, vol. 66, no. 10, pp. 1444–1454, 2006.

[24] A. S. Kaddour, M. J. Hinton, P. A. Smith, and S. Li, "A comparison between the predictive capability of matrix cracking, damage and failure criteria for fibre reinforced composite laminates: Part A of the third world-wide failure exercise," *Journal of Composite Materials*, vol. 47, no. 20-21, pp. 2749–2779, 2013.

[25] C. C. Chamis, F. Abdi, M. Garg, L. Minnetyan, H. Baid, D. Huang, J. Housner, and F. Talagani, "Micromechanics-based progressive failure analysis prediction for WWFE-III composite coupon test cases," *Journal of Composite Materials*, vol. 47, no. 20-21, pp. 2695–2712, 2013.

[26] F. Laurin, N. Carrere, C. Huchette, and J. F. Maire, "A multiscale hybrid approach for damage and final failure predictions of composite structures," *Journal of Composite Materials*, vol. 47, no. 20-21, pp. 2713–2747, 2013.

[27] M. Kashtalyan and C. Soutis, "Predicting residual stiffness of cracked composite laminates subjected to multi-axial inplane loading," *Journal of Composite Materials*, vol. 47, no. 20-21, pp. 2513–2524, 2013.

[28] P. A. Carraro and M. Quaresimin, "A stiffness degradation model for cracked multidirectional laminates with cracks in multiple layers," *International Journal of Solids and Structures*, vol. 58, pp. 34–51, 2015. [Online]. Available: http://linkinghub.elsevier.com/retrieve/pii/S0020768314004843

[29] J. A. Glud, J. M. Dulieu-Barton, O. T. Thomsen, and L. C. T. Overgaard, "A stochastic multiaxial fatigue model for off-axis cracking in FRP laminates," *International Journal of Fatigue*, vol. 103, pp. 576–590, 2017. [Online]. Available: http://dx.doi.org/10.1016/j.ijfatigue.2017.06.012

[30] J. Zangenberg, P. Brøndsted, and J. W. Gillespie, "Fatigue damage propagation in unidirectional glass fibre reinforced composites made of a non-crimp fabric," *Journal of Composite Materials*, vol. 48,

no. 22, pp. 2711–2727, 2013. [Online]. Available: http://jcm.sagepub.com/content/48/22/2711.short
[31] K. M. Jespersen, J. Zangenberg, T. Lowe, P. J. Withers, and L. P. Mikkelsen, "Fatigue damage assessment of uni-directional non-crimp fabric reinforced polyester composite using X-ray computed tomography," *Composites Science and Technology*, vol. 136, pp. 94–103, 2016. [Online]. Available: http://dx.doi.org/10.1016/j.compscitech.2016.10.006
[32] S. Korkiakoski, E. Sarlin, R. Suihkonen, and O. Saarela, "Influence of reinforcement positioning on tension-tension fatigue performance of quasi-unidirectional GFRP laminates made of stitched fabrics," *Composites Part B: Engineering*, vol. 112, pp. 38–48, 2017. [Online]. Available: http://dx.doi.org/10.1016/j.compositesb.2016.12.017
[33] D. Ashouri Vajari, B. N. Legarth, B. F. Sørensen, C. F. Niordson, and C. Berggreen, "Micromechanical failure in fiber-reinforced composites," Ph.D. dissertation, DTU Mechanical Engineering, 2014.
[34] L. Maragoni, P. A. Carraro, M. Peron, and M. Quaresimin, "Fatigue behaviour of glass/epoxy laminates in the presence of voids," *International Journal of Fatigue*, vol. 95, pp. 18–28, 2017. [Online]. Available: http://dx.doi.org/10.1016/j.ijfatigue.2016.10.004
[35] H. Shen, W. Yao, W. Qi, and J. Zong, "Experimental investigation on damage evolution in cross-ply laminates subjected to quasi-static and fatigue loading," *Composites Part B: Engineering*, vol. 120, pp. 10–26, 2017. [Online]. Available: http://dx.doi.org/10.1016/j.compositesb.2017.02.033
[36] Z. Sun, I. M. Daniel, and J. J. Luo, "Modeling of fatigue damage in a polymer matrix composite," *Materials Science and Engineering A*, vol. 361, no. 1-2, pp. 302–311, 2003.
[37] M. C. Lafarie-Frenot and C. Hénaff-Gardin, "Formation and Growth of 90° Ply Fatigue Cracks in Carbon/Epoxy Laminates," *Composites Science and Technology*, vol. 40, no. 3, pp. 307–324, 1991.
[38] K. W. Garrett and J. E. Bailey, "Multiple transverse fracture in 90° cross-ply laminates of a glass fibre-reinforced polyester," *Journal of Materials Science*, vol. 12, no. 1, pp. 157–168, 1977.